

<https://doi.org/10.17488/RMIB.44.4.8>

E-LOCATION ID: 1396

## Development of an Adaptive Acquisition and Transmission System for Digital Processing of ECG Signals under Variable n-QAM Schemes

### Desarrollo de un Sistema Adaptativo de Adquisición y Transmisión para el Procesamiento Digital de Señales de ECG Bajo Esquemas Variables n-QAM

José Ricardo Cárdenas-Valdez<sup>1</sup>, Fortunato Ramírez-Arzate<sup>1</sup>, Angel Humberto Corral-Domínguez<sup>1</sup>,  
Carlos Hurtado-Sánchez<sup>1</sup>, Andrés Calvillo-Téllez<sup>2</sup>, Enrique Efrén García-Guerrero<sup>3</sup>

<sup>1</sup>Tecnológico Nacional de México - Instituto Tecnológico de Tijuana, Baja California - México

<sup>2</sup>Instituto Politécnico Nacional - CITEDI, Baja California - México

<sup>3</sup>Universidad Autónoma de Baja California, Baja California - México

#### ABSTRACT

In the post-pandemic era, it is critical to monitor and transmit biomedical signals, specifically ECG. This study aims to develop a platform that enables signal acquisition, adaptation, and transmission using different n-QAM modulation schemes. The system comprises an acquisition stage implemented in the 2.5 GHz band employing the Olimex module and electrodes equipped with an Ag/AgCl type sensor. To effectively manage appropriate bandwidths during implementation of the various n-QAM modulation schemes, an adaptive algorithm was developed and applied to the system. The power amplifier was operated in the linear region to enhance the crest factor and achieve an ACPR close to 30 dBc, demonstrating an appropriate demodulation of the electrocardiogram (ECG) signal, it is feasible to shift to modulation schemes above 64-QAM in order to detect high frequencies and perform a subsequent Fourier analysis. As a telemedicine proposal, the developed system offers flexibility in signal acquisition, data storage, and digitalization, in addition to a multivariable n-QAM scheme; the hardware implementation ensures n-QAM scheme compatibility. For the purpose of contributing to telemedicine via RF transmission, the system was executed on an AD9361 transceiver, which removes the requirement for a traditional signal vector generator and enables optimal control of the tones to be transmitted.

**KEYWORDS:** ECG, n-QAM, RF, telemedicine, transceiver

## RESUMEN

El monitoreo y transmisión de señales biomédicas, particularmente ECG, es fundamental en la era pospandemia, este trabajo de investigación se centra en el desarrollo de una plataforma para la adquisición, adaptación y transmisión de señales bajo diversos esquemas de modulación n-QAM. El sistema incluye una etapa de adquisición mediante el módulo Olimex y electrodos con un sensor tipo Ag/AgCl. Se desarrolló un algoritmo adaptativo a los diversos esquemas de modulación n-QAM para la gestión de anchos de banda apropiados durante una implementación en la banda de 2,5 GHz, al amplificador de potencia se operó en la región lineal para mejorar el factor de cresta y obtener un ACPR cercano a 30 dBc, se realizó una demodulación adecuada de la señal ECG y es posible migrar a esquemas de modulación superiores a 64-QAM si se requiere detectar altas frecuencias y un posterior análisis de Fourier. El sistema desarrollado como propuesta de Telemedicina brinda versatilidad para la adquisición de señales, digitalización, almacenamiento de datos y un esquema multivariable n-QAM, la implementación en hardware proporcionó una adecuada adaptabilidad para esquemas n-QAM. El sistema se implementó sobre un transceptor AD9361 que elimina el tradicional generador vectorial de señal y permite un control óptimo de los tonos a enviar, para aporte en el área de Telemedicina a través de transmisión RF.

**PALABRAS CLAVE:** ECG, n-QAM, RF, telemedicina, transceptor

### Corresponding author

TO: José Ricardo Cárdenas-Valdez

INSTITUTION: Tecnológico Nacional de México/Instituto Tecnológico de Tijuana

ADDRESS: Blvd. Industrial s/n, Cd Industrial, C.P. 22430, Tijuana, Baja California.

EMAIL: jose.cardenas@tectijuana.edu.mx

### Received:

31 oct 2023

### Accepted:

07 dic 2023

## INTRODUCTION

Cardiovascular disease is a significant contributor to mortality on a global scale, it is estimated that a third of the causes of death in the world are related to this cardiovascular diseases <sup>[1]</sup>; in addition to the critical nature of detecting cardiac abnormalities for preventive treatment, the rapid growth of telemedicine development since 2021 as a result of the pandemic further emphasizes this fact, despite the fact that the most significant contributions to this field are older than ten years. Telemedicine faces obstacles, especially in the digital field, connectivity systems, and access to devices. In addition, the learning curve of the diverse range of accessories for sensing and transmission, the most crucial challenge is adopting digital technologies, especially for specialized systems such as radio frequency (RF), and Internet of things (IoT) as the main employed methods in high data rate transmissions <sup>[2][3]</sup>. The electrocardiogram (ECG) signal analysis is used in various study cases, particularly in people who require constant monitoring of heart rhythms, postoperative monitoring, or high-performance athletes, all of them to detect any pathology or measurement in the time domain of PQ, QRS or QT intervals <sup>[4][5]</sup>. A biomedical application is devised in <sup>[6]</sup> that utilizes flexible electrodes to enable field communication that is compatible with digital stages. Previous work has examined the feasibility of wirelessly transmitting biomedical signals using the long-term evolution (LTE) standard. Additionally, for the 3rd Generation Partnership Project (3GPP), a proposition was placed forth to reduce latency on machine-type communication technology <sup>[7]</sup>. Additionally, detection based on ECG signals is a current challenge, especially for the development of classifiers and detection of cardiac arrhythmia; the process of transmitting signals wirelessly and maintaining the originality of the acquired signal is crucial in diagnosis <sup>[8][9]</sup>. A fundamental aspect of biomedical applications is spectral analysis, which is utilized to identify and invade adjacent bands or to implement in free bands during radio frequency (RF) transmissions <sup>[10]</sup>. To reduce the power consumption of synthetic data

obtained from the PhysionNet database, an embedded application and a study based on fast Fourier transform (FFT) were created <sup>[11]</sup>.

Digital multiplexes such as orthogonal frequency-division multiplexing (OFDM) have been adopted as a basis in state-of-the-art work in 4G-5G applications. In addition to transmission standards such as LTE, the benefits of OFDM multiplexes are sub-channeling efficiency for handling multipath fading channels and, and consequently efficient per-tone multiple-input multiple-output (MIMO) processing support <sup>[12]</sup>.

A reconfigurable system designed to reduce energy consumption is presented in <sup>[13]</sup>. This system finds utility in biomedical contexts, specifically in the transmission of quadrature amplitude modulation (QAM), frequency shift keying (FSK), and phase shift keying (PSK), unfortunately additional biomedical information is required to validate the developed system. The development of Telemedicine applications in 5th generation (5G) networks in the post-pandemic era is a key factor for advancements in RF performance <sup>[14][15]</sup>; in <sup>[16]</sup> is presented an ECG monitor scheme with two-stage end-to-end improving the power consumption. Additionally, the implementation of high-efficiency amplifiers for large signals under 64-QAM enables the processing of large amounts of data in 5G applications <sup>[17]</sup>.

ECG monitoring offers remote control of acquired data and provides continuous and remote surveillance of patients <sup>[18]</sup>. This research endeavor provides a proposal for hardware implementation and analysis in the frequency domain of ECG signal monitoring employing n-QAM schemes in the 2.5 GHz band, In the post-pandemic era, examine the spectral purity of an RF transmission for telemedicine applications by evaluating figures of merit and ensuring an appropriate adjacent channel power ratio (ACPR).

This work is organized as follows: Section 2 describes

the proposed testbed and digitization stage and the adaptive algorithm. Section 3 shows the results of the hardware implementation in the transceiver. Section 4 summarizes the conclusions of the paper.

## MATERIALS AND METHODS

### n-QAM adaptive system

Digital multiplexes such as OFDM have been adopted as a basis in state-of-the-art work in 4G-5G applications. In addition to transmission standards like LTE, OFDM multiplexes exhibit inherent benefits that have been particularly developed in [12], extend sub-channeling efficiency, a critical characteristic when handling multipath fading channels. OFDM multiplexes enable effective support to per-tone MIMO processing [12]. With the development of 5G exponentially worldwide, the need to use high transfer rate schemes and multimedia applications, as well as lower resource consumption, the modulation scheme to be used plays a crucial role in the management of wide band bandwidth and power efficiency [19]. N-QAM schemes are used in modern communication standards due to flexibility in bandwidth management and power efficiency [20]. QAM is adaptable and versatile enough to be utilized in the sub-channeling and utilization of information within multiplexation such as OFDM. In the Figure 1 is depicted an example of 64-QAM scheme.

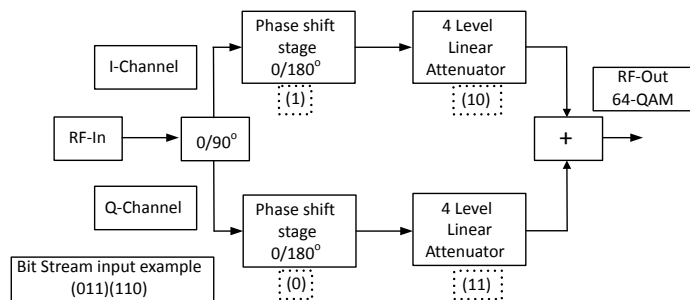


FIGURE 1. Overview of a typical 64-QAM modulator.

In this research work, an adaptable n-QAM scheme is formulated for the purposes of acquiring and preprocessing ECG signals. Within this framework, two chan-

nels I and Q, are assumed, whose symbol packaging is of the type Equation (1) and Equation (2).

$$a_k = a_k I + j a_k I, \quad (1)$$

$$b_k = b_k I + j b_k I. \quad (2)$$

The parameters  $a_k$  and  $b_k$  represent the amplitudes corresponding to the  $k$ -th symbols within the in-phase (I) and quadrature (Q) channels, respectively. In the context of n-QAM modulation systems, the values of  $a_k$  and  $b_k$  are selected from the set  $\{2i - 1 - f\sqrt{n}\}$  where  $f$  takes on values within the range  $f = \{1, \dots, \sqrt{n}\}$ . Here,  $f$  serves as a parameter defining the n-QAM constellation, as expressed by Equation (3):

$$d = \sqrt{\frac{[3 \log_2(M) E_b]}{2(n-1)}}. \quad (3)$$

In this context,  $E_b$  represents the energy per bit, and the per-bit sequence derived from n-QAM is characterized by  $c_k$ , denoted as the sequence, with  $w_k$  representing the pilot sequence. The factor  $\alpha$  is intricately linked to the power ratio between the proposed pilot sequence  $w_k$  and the power associated with the information sequence  $b_k$ . It is posited that  $w_k$  assumes the form of a periodic sequence of  $N_s$ , where the period  $T_w$  is equal to  $N_s T_s$ . The transmitted n-QAM signal is represented in accordance with conventions established by [21][22], denoted by Equation (4).

$$s(t) = \sum c_n p(t - nT_s), \quad (4)$$

where  $p(t)$  is the pulse waveform associated with the transmission process and in the presence of multipath propagation and noise the signal  $z(t)$  depicted by Equation (5) is received:

$$z(t) = \sum c_n q(t - nT_s) + u(t), \quad (5)$$

In this stage  $q(t)$  the signal filtering stages are taken into account, both the one used in the transmission and reception.

An additional metric of considerable import to assess during the implementation phase is the ACPR. It delineates the power ratio within a telecommunications system by discerning the power in the adjacent channels relative to that within the main bandwidth. ACPR assumes a pivotal role as a primary analytical metric in telecommunications systems, since it evaluates the level of interference that the transmission has in its main bandwidth concerning other bands. In this context, augmenting the ACPR level is imperative to ensure the efficacy of the transmission process. ACPR is represented mainly by Equation (6) involving the Third Order Intercept Point (IP3) and Equation (7) by the average power of the main channels against the adjacent channels.

$$ACPR = -20.75 + 160 \log \left( \frac{P_{ref}}{P_{adj}} \right) + 2(P_{in} - IP3), \quad (6)$$

$$ACPR(dBc) = 10 \log_{10} \left( \frac{P_{ref}}{P_{adj}} \right), \quad (7)$$

where  $P_{ref}$  is the average power of the main bandwidth,  $P_{adj}$  is the average power of the adjacent bands, the crest factor (CF) can also be defined as the power ratio between  $P_{ref}$  and  $P_{adj}$ .

Figure 2 delineates the spectral distribution of frequency bands, and the average power of the main bandwidth, as well as the adjacent bands. The ACPR serves as a crucial merit figure for assessing the potential for interference with adjacent bands. It is employed to ascertain compliance with regulatory standards, such as those stipulated by the standard for Telecommunications IEEE 802.n [23], to validate that the spectral growth is below the limits established by the FCC. The ACPR, measured in decibels relative to the carrier (dBc), assumes particular significance in the

context of mitigating undesirable effects arising from memory and linearity issues inherent in the transmitter stage. This is particularly pertinent to distortions induced by the RF-power amplifier. A robust ACPR value, approaching or exceeding 30 dBc, ensures that unwanted memory and linearity effects of the transmitter stage, particularly those induced by the RF-Power amplifier, have been eliminated.

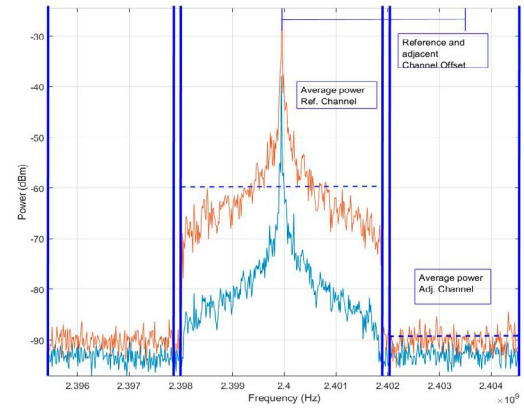


FIGURE 2. Band distribution for ACPR calculation.

### ECG acquisition data and RF transmission

The block diagram of the experimental setup is depicted in Figure 3, outlines in the beginning the procedure for obtaining a precordial signal, establishing an AVR: Existence of net potential on the right (aVr), net potential existing on the left side (aVl). and voltage reference (AVF) type lead placement to form the Einthoven triangle for acquiring P, QRS, and T waves [24]. In this case, the used electrodes include polyethylene, they are biocompatible, coated with acrylic copolymer, with an AgCl type sensor; conductive gel was placed on the terminal to improve the acquisition of the ECG signal. In the acquisition stage, an Olimex module is used coupled to the digital I/O port with the Arduino Uno embedded system; the design was built in C++ language in a Java environment. The storage between boards allows heart peak detection, calculation of sample based heart rate, and adequate accuracy of the extracted biomedical signals.

Variations in the magnitude of voltage compensation,

amplitude variation, and data array length obtained by the embedded system ECK/EKG board are accounted for in an adaptive stage of Algorithm 1. The algorithm commences by establishing a m-ary number associated with the defined QAM modulation scheme. It then proceeds to identify the length of the array and normalizes it to a unitary amplitude, which is subsequently processed by the AD9361 Toolkit. Furthermore, it supports an amplitude range of 2 to 12 for one of the  $2 \times 2$  channels transceivers that incorporate a 12-bit DAC and ADC. In the M programming language, the digitized and transmitted signal is stored as an environment variable. The data to be transmitted and before demodulation is packaged in n-QAM order packets. The demodulated signal is subsequently encoded as a variable within a Matlab environment. This enables mathematical classifiers for biomedical signals and analysis in the frequency domain.

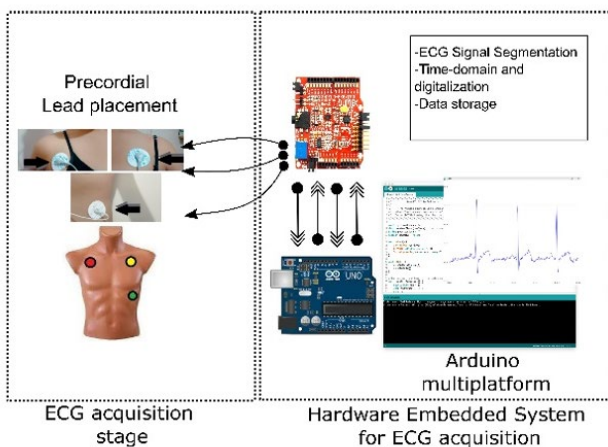


**FIGURE 3. ECG acquisition within an embedded multiplatform.**

As an intermediate stage, the ECG signal segmentation process is carried out based on Algorithm 1, and storage of the digitized variables in the processing of the data to operate the FMCOMMS3 RF transceiver, a variable n-QAM stage is designed; the characteristics of bandwidth (BW), gain mode sampling frequency are adjusted in the AD9361 transceiver toolkit, the transmitter stage comprises an n-QAM modulator, coupled with a raise cosine filter coupled prior to transmission in Matlab environment.

**ALGORITHM 1. ECG signal segmentation and n-QAM digital packets.**

```

Require:  $n \geq 1$ 
Ensure:  $ECG_{QAM} = ECG_{stream}/n$ 
while  $N = 0$  and  $N \leq \text{length}(ECG_{dq})$  do
  if  $N$  is integer then
     $ECG_{offset} = ECG_{dq} - \min(ECG_{dq})$ 
     $ECG_{norm} = ECG_{offset}/\max(ECG_{dq})$ 
     $ECG_{stream} = \text{Dec2Bin}(ECG_{norm})$ 
  end if
  StoreDigitalizedSignal  $\leftarrow$   $ECG_{stream}$ 
end while

```

In this work, an RF power amplifier ZX60-5916MA-S+ is used as a device under test (DUT); it is a proper device for ultra-wide band applications when is required high linearity, including the 2.5 GHz band, it improves lower system noise figure performance. The transceiver used has a carrier frequency of 2.45 GHz, the ARRadio card includes the AD9361 transceiver, the modulator system is variable at n-QAM levels. In this case, quadrature phase shift keying (QPSK) was used as the fundamental modulation into the Cyclone V FPGA SoC-Kit development board. The development board provides full control of the transmitted tones, which replaces the traditional signal vector generator (SVG), and the RF transmission is validated in the Spectrum Analyzer SSA-3032X. The testbed is protected due to the coupled port attenuation of -20.73 and the attenuator BW-S10W5+ of 10 dB. The directional coupler as a passive device provides high isolation between the medium power levels and the digital schemes, improving the reflected signal transmitted signal.

Figure 4 delineates the schematic representation of the digitization stage, baseband adaptation, and digital modulation processes, data preprocessing procedures that precede the transmission through the AD9361 transceiver. Furthermore, the signal is directed to a ZFBP-2400-S+ low-pass filter designed for operation within the 2.5 GHz band. A directional coupler, specifically the ZHDC-16-63-S+, is employed to mitigate line

feedback and suppress spurious noise within the system. Notably, the RF power amplifier as a device under test is the RF-PA ZX60-5916MA-S+. Concurrently, a spectral evaluation of the transmission is carried out using the SSA 3032X spectrum analyzer.

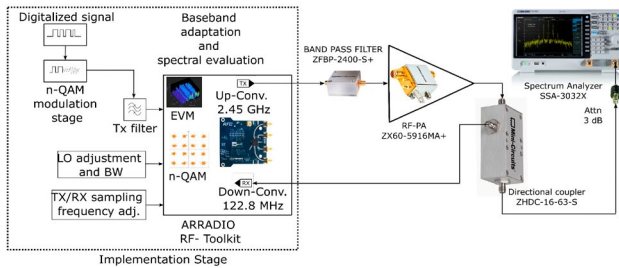


**FIGURE 4. Schematic representation of digitization, baseband adaptation and transmission of the AD9361 transceiver.**

Figure 5 depicts the devised test bench designed for the comprehensive handling of data storage, preprocessing, and transmission processes, inclusive of the AD9361 RF Agile Transceiver + FPGA-SocKit transceiver. The ARRADIO board, serving as a pivotal component, is purposed to furnish a platform for RF full-tone control. In this specific instantiation, a balun operating within the 2.4-2.5 GHz ranges is employed. The utilization of advanced transceivers enables precise tone regulation, obviating the need for expensive SVR. Furthermore, this setup facilitates the discretization, storage, and processing of data.

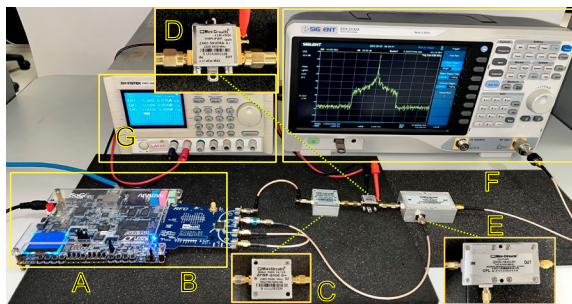


**FIGURE 5. Overview of the developed experimental testbed. (A-B) AD9361 RF Agile Transceiver + FPGA-SocKit. (C) ZFBP-2400-S+ 50Ω Narrow bandpass Filter. (D) ZX60-5916MA-S+ RF-Power Amplifier. (E) ZHDC-16-63-S+ Directional Coupler. (F) Spectrum Analyzer SIGLENT SSA3032X.**

In the hardware transmission stage, a ZFBP-2400-S+ 50Ω narrow-bandpass filter is integrated, with a pronounced rejection capability of 50 dB, affording protective measures against undesired transmissions in the sidebands. Subsequently, in the intermediate stage, a ZHDC-16-63-S+ high directivity directional coupler is employed, characterized by superior coupling flatness and providing requisite attenuation to mitigate line return effects during the transmission process.

## RESULTS AND DISCUSSION

One of the main challenges of Telemedicine applications through RF transmission is the low nonlinearity involved in the transmitter stage; a critical consideration is to ensure that biomedical signals operate within power regimes below the P1dB threshold, thereby mitigating intrinsic nonlinearities. The RF-PA model ZX60-5916MA-S+ operates under the P1dB threshold of 10.63 dBm, ensuring heightened linearity without compromising power during RF transmission. The active directivity of the DUT particularly suitable for minimizing noise in the receiver stage and facilitating the recovery of the demodulated signal.

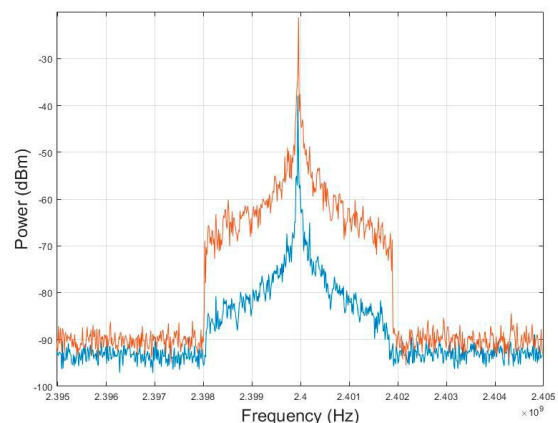


**FIGURE 6. Spectral analysis of the acquired ECG signal compared to that amplified by the DUT.**

Figure 6 illustrates the relation between input power and output power, emphasizing the utilization of the RF-PA within its linear operational range for optimal

power efficiency in telemedicine transmission applications. At the central point of the bandwidth, a power level of -27.9 dBm is noted, while the output power is reached at -11.2 dBm, resulting in the DUT operating with a gain of 16.7 dB.

Figure 7 depicts the acquired signal derived from the embedded ECG/EKG board, wherein the system comprises an acquisition stage utilizing the Olimex module in conjunction with electrodes featuring an AgCl-type sensor. An algorithm has been devised for the discernment of peaks within cardiac signals, facilitating the determination of heart rate, and the subsequent computation of sample-based heart rate.

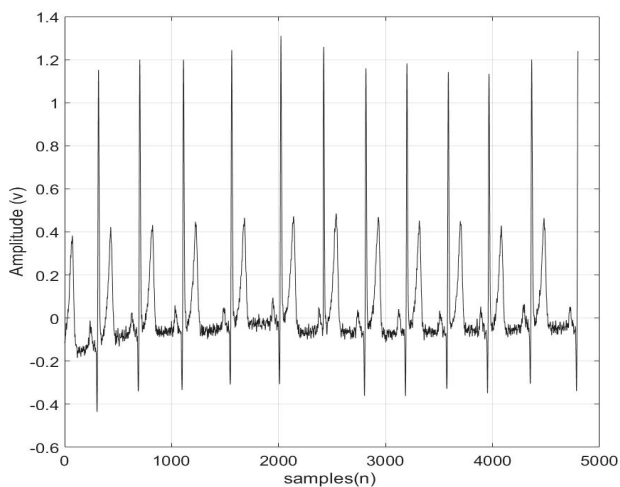


**FIGURE 7. signal recovered in the time domain under that 32-QAM modulation scheme.**

Figure 8 presents the signal recuperated under the 16-QAM scheme, wherein each cycle comprises 16 constituent parts constituting the signal. It is noteworthy that despite the 4-bit packaging characteristic of 16-QAM, the scheme leverages speed advantages during the transmission process. Subsequently, Figure 9 illustrates the signal recovery under the 32-QAM modulation scheme, involving a discretization of 32 segments and a packaging configuration of 5 bits per event.

In addition, the 64-QAM modulation scheme is illustrated, (Figure 10), featuring a significant discretiza-

tion of the signal and an enhancement of -20 dB in the NMSE. It has been determined that the integration of higher-order n-QAM schemes into subsequent procedures may have the potential to improve NMSE, particularly when high induced frequencies in the signal are required for Fourier domain analysis.

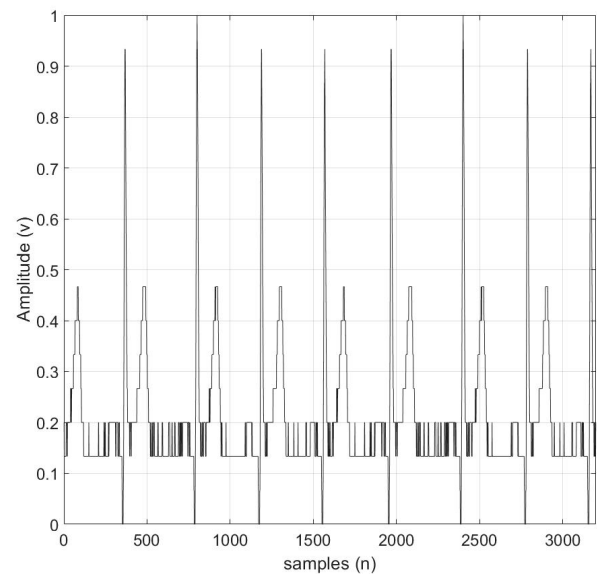


**FIGURE 8. The time domain signal recovered by the 16-QAM modulation scheme.**

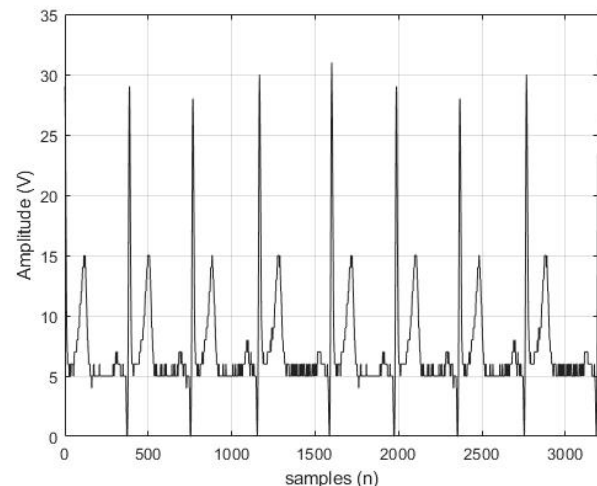


**FIGURE 9. The time domain signal recovered by the 32-QAM modulation scheme.**

Spectral validation is critical to ensure that there is no invasion of adjacent bands during the transmission process; ACPR is a figure of primary merit for this anal-

ysis since it defines the relationship of the average power between the main bandwidth and the side channels, the signal is shown in Figure 11; acquired from the transmitter showing -27.89 dBm due to the 10 dB attenuator located at the input port of the Spectrum Analyzer SIGLENT SSA3032X, and Figure 12 shows the signal amplified by the DUT ZX60-5916MA-S+ with a power of -11.21 dBm given that it passes through the 10 dB attenuator of the input port.

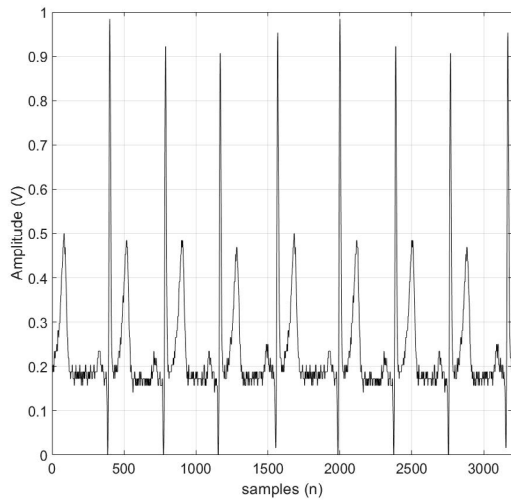


**FIGURE 10.** The time domain signal recovered by the 64-QAM modulation scheme.

Table 1 describes the metrics achieved during the implementation. A bandwidth of 10 MHz is used because the transmission of ECG signals involves a relatively low level of BW for digital modulation, which provides flexibility to migrate to higher bandwidths if the monitoring of several biomedical signals and transmission is required, a crest factor of 718.85 is obtained showing an appropriate relationship of the main BW concerning the power of the adjacent bands, the achievement of an ACPR of 28.56 dBc enables the implementation of modulation schemes that ensure the highest order n-QAM.

**TABLE 1. Power spectral validation**

RF-PA spectral validation	
Average power of main BW	-61.546 dBm
Average power of the adjacent channel	-90.112 dBm
Crest Factor	718.85
BW power validation	$7.005 \times 10^{-7}$ mW
Adjacent channels power validation	$9.745 \times 10^{-10}$ mW
ACPR	28.56 dBc
BW	10 MHz

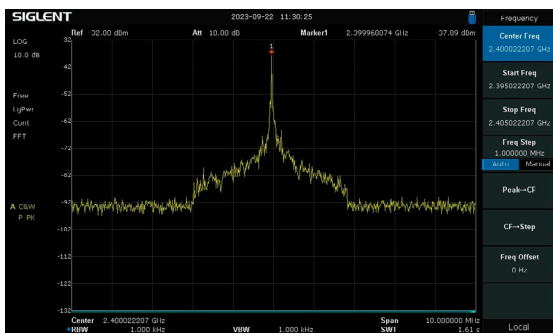


**FIGURE 11.** Transmitted stimulus under a 10 dB attenuation.

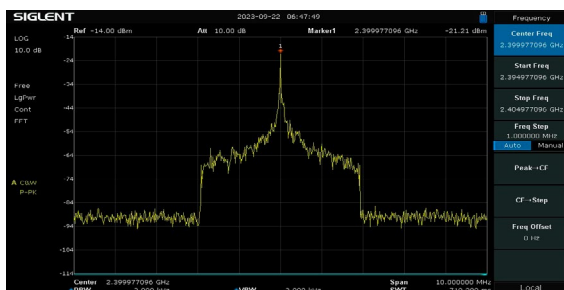


**FIGURE 12.** Amplified signal under a 10 dB attenuation.

## CONCLUSIONS

This research work introduces a substantive contribution to the field of Telemedicine, characterized by key stages encompassing signal acquisition facilitated by an Olimex module along with electrodes featuring an AgCl-type sensor. Additionally, a M-language algorithm is formulated for the segmentation and storage of biomedical signals. The digitized ECG signal undergoes modulation utilizing a variable n-QAM scheme, with a designated bandwidth of 10 MHz chosen to accommodate the periodic nature of the signals during transmission. By selecting this option, the crest factor is decreased, which encourages the consideration of implementing higher QAM schemes. The application of n-QAM modulation transcends ECG signals and facilitates the transmission of real-time data while managing a wide variety of biological signals.

The transceiver system's intrinsic regulation of the transmission process eliminates the need for expensive signal vector generators in the laboratory, thereby guaranteeing accuracy during signal acquisition, pre-processing, and data transmission. In addition, a flexible algorithm is developed for handling various n-QAM orders in order to discretize, store, and package data within the OFDM framework.

The transition of systems to 5G requires the implementation of adaptive platforms that are capable of meeting digital modulations, consume just the necessary bandwidth, and follow the crest factor and ACPR limits. These limits are imposed by the RF power amplifier being evaluated, which is susceptible to spectral growth resulting from nonlinearities and memory effects.

The platform and algorithm developed are an alternative in Telemedicine applications because they allow the acquisition of biomedical signals and wireless transmission, especially in rural areas where the doctor is located remotely or his location is centralized for monitoring several towns.

### **AUTHOR CONTRIBUTIONS**

J.R.C.V. developed the methodology, participated in the design and development of the algorithms used, oversaw the experiments and participated in the analyses of results. F.R.A. participated in the data gathering and processing, use of specialized software. A.H.C.D. developed hardware and software for data gathering. C.H.S. design and developed programming language and code for data gathering and analysis. A.C.T. design and developed algorithms for data gathering and validated data. E.E.G.G. validated data and results for the discussion. All authors participated in all the writing stages of the manuscript, reviewed and approved the final version of the manuscript.

## REFERENCES

- [1] World Health Organization, "Cardiovascular diseases (CVDs)," WHO. 2021. [Online]. Available: [https://www.who.int/news-room/fact-sheets/detail/cardiovascular-diseases-\(cvds\)](https://www.who.int/news-room/fact-sheets/detail/cardiovascular-diseases-(cvds))
- [2] A. Ibaida, A. Abuadba, N. Chilamkurti, "Privacy-preserving compression model for efficient IoMT ECG sharing," *Comput. Commun.*, vol. 166, no. 15, pp. 1-8, Jan. 2021, doi: <https://doi.org/10.1016/j.comcom.2020.11.010>
- [3] C. De Capua, A. Meduri and R. Morello, "A Smart ECG Measurement System Based on Web-Service-Oriented Architecture for Telemedicine Applications," *IEEE Trans. Instrum. Meas.*, vol. 59, no. 10, pp. 2530-2538, Oct. 2010, doi: <https://doi.org/10.1109/TIM.2010.2057652>
- [4] J. Francis, "ECG monitoring leads and special leads," *Indian Pacing Electrophysiol. J.*, vol. 16, no. 3, pp. 92-95, 2016, doi: <https://doi.org/10.1016/j.ipej.2016.07.003>
- [5] I. -A. Ivanciu, L. Ivanciu, D. Zinca, and V. Dobrota, "Securing Health-Related Data Transmission Using ECG and Named Data Networks," in 2019 IEEE International Symposium on Local and Metropolitan Area Networks (LANMAN), Paris, France, 2019, pp. 1-6, doi: <https://doi.org/10.1109/LANMAN.2019.8846993>
- [6] M. Zulqarnain, S. Stanzone, G. Rathinavel, S. Smout, M. Willegems, K. Myny, and E. Cantatore, "A flexible ECG patch compatible with NFC RF communication," *npj Flex. Electron.*, vol. 4, art. no. 13, Jul. 2020, doi: <https://doi.org/10.1038/s41528-020-0077-x>
- [7] Y. Cho, H. Shin, and K. Kang, "Scalable Coding and Prioritized Transmission of ECG for Low-Latency Cardiac Monitoring Over Cellular M2M Networks," *IEEE Access*, vol. 6, pp. 8189-8200, Jan. 2018, doi: <https://doi.org/10.1109/ACCESS.2018.2795028>
- [8] N. Clark, E. Sandor, C. Walden, I. S. Ahn and Y. Lu, "A wearable ECG monitoring system for real-time arrhythmia detection," in 2018 IEEE 61st International Midwest Symposium on Circuits and Systems (MWSCAS), Windsor, ON, Canada, 2018, pp. 787-790, doi: <https://doi.org/10.1109/MWSCAS.2018.8624097>
- [9] G. Cosoli, S. Spinsante, F. Scardulla, L. D'Acquisto and L. Scalise, "Wireless ECG and cardiac monitoring systems: State of the art, available commercial devices and useful electronic components," *Measurement*, vol. 177, art. no. 109243, Jun. 2021, doi: <https://doi.org/10.1016/j.measurement.2021.109243>
- [10] S. M. Noor, E. John, and M. Panday, "Design and Implementation of an Ultralow-Energy FFT ASIC for Processing ECG in Cardiac Pacemakers," *IEEE Trans. Very Large Scale Integr. VLSI Syst.*, vol. 27, no. 4, pp. 983-987, Apr. 2019, doi: <https://doi.org/10.1109/TVLSI.2018.2883642>
- [11] A. L. Goldberger, L. A. Amaral, L. Glass, J. M. Hausdorff, et al., "PhysioBank, PhysioToolkit, and PhysioNet: Components of a new research resource for complex physiologic signals," *Circulation*, vol. 101, no. 23, pp. e215-e220, 2000, doi: <https://doi.org/10.1161/01.cir.101.23.e215>
- [12] C. Kim, Y. H. Yun, K. Kim, and J. -Y. Seol, "Introduction to QAM-FBMC: From Waveform Optimization to System Design," *IEEE Commun. Mag.*, vol. 54, no. 11, pp. 66-73, Nov. 2016, doi: <https://doi.org/10.1109/MCOM.2016.1600384CM>
- [13] C. -H. Heng and K. -H. Teng, "Reconfigurable, energy efficient transmitter with band-shaping and multi-channel support for biomedical applications," in 2016 URSI Asia-Pacific Radio Science Conference (URSI AP-RASC), Seoul, Korea (South), 2016, pp. 986-989, doi: <https://doi.org/10.1109/URSIAP-RASC.2016.7601308>
- [14] B. O. hAnnaidh, P. Fitzgerald, H. Berney, R. Lakshmanan, N. Coburn, S. Geary, B. Mulvey, "Devices and Sensors Applicable to 5G System Implementations," in 2018 IEEE MTT-S International Microwave Workshop Series on 5G Hardware and System Technologies (IMWS-5G), Dublin, Ireland, 2018, pp. 1-3, doi: <https://doi.org/10.1109/IMWS-5G.2018.8484316>
- [15] T.-H. Tsai and W.-T. Kuo, "An Efficient ECG Lossless Compression System for Embedded Platforms With Telemedicine Applications," *IEEE Access*, vol. 6, pp. 42207-42215, Jul. 2018, doi: <https://doi.org/10.1109/ACCESS.2018.2858857>
- [16] N. Wang, J. Zhou, G. Dai, J. Huang, and Y. Xie, "Energy-Efficient Intelligent ECG Monitoring for Wearable Devices," *IEEE Trans. Biomed. Circuits Syst.*, vol. 13, no. 5, pp. 1112-1121, Oct. 2019, doi: <https://doi.org/10.1109/TBCAS.2019.2930215>
- [17] K. Nakatani, Y. Yamaguchi, Y. Komatsuzaki, S. Sakata, S. Shinjo, and K. Yamanaka, "A Ka-Band High Efficiency Doherty Power Amplifier MMIC using GaN-HEMT for 5G Application," in 2018 IEEE MTT-S International Microwave Workshop Series on 5G Hardware and System Technologies (IMWS-5G), Dublin, Ireland, 2018, pp. 1-3, doi: <https://doi.org/10.1109/IMWS-5G.2018.8484612>
- [18] D. Lucani, G. Cataldo, J. Cruz, G. Villegas, and S. Wong, "A portable ECG monitoring device with Bluetooth and Holter capabilities for telemedicine applications," in 2006 International Conference of the IEEE Engineering in Medicine and Biology Society, New York, NY, USA, 2006, pp. 5244-5247, doi: <https://doi.org/10.1109/IEMBS.2006.260798>
- [19] P. K. Singya, P. Shaik, N. Kumar, V. Bhatia, and M.-S. Alouini, "A Survey on Higher-Order QAM Constellations: Technical Challenges, Recent Advances, and Future Trends," in *IEEE Open J. Commun. Soc.*, vol. 2, pp. 617-655, 2021, doi: <https://doi.org/10.1109/OJCOMS.2021.3067384>
- [20] T. S. Rappaport, *Wireless Communications: Principles and Practice*, vol. 2. Upper Saddle River, NJ, USA: Prentice-Hall PTR, 1996.
- [21] F. Mazzenga, "Channel estimation and equalization for M-QAM transmission with a hidden pilot sequence," *IEEE Trans. Broadcast.*, vol. 46, no. 2, pp. 170-176, 2000, doi: <https://doi.org/10.1109/11.868934>
- [22] J. G. Proakis and M. Salehi, *Digital Communications*, 2nd ed. NJ, USA: McGraw-Hill, Higher education, 2008.
- [23] "IEEE Standard for Telecommunications and Information Exchange Between Systems - LAN/MAN Specific Requirements - Part 11: Wireless Medium Access Control (MAC) and physical layer (PHY) specifications: High Speed Physical Layer in the 5 GHz band," in *IEEE Std 802.11a-1999*, pp.1-102, 1999, doi: <https://doi.org/10.1109/IEEESTD.1999.90606>
- [24] B. Abi-Saleh, B. Omar, "Einthoven's Triangle Transparency: A Practical Method to Explain Limb Lead Configuration Following Single Lead Misplacements," *Rev. Cardiovasc. Med.*, vol. 11, no. 1, pp. 33-38, 2010, doi: <https://doi.org/10.3909/ricm0506>